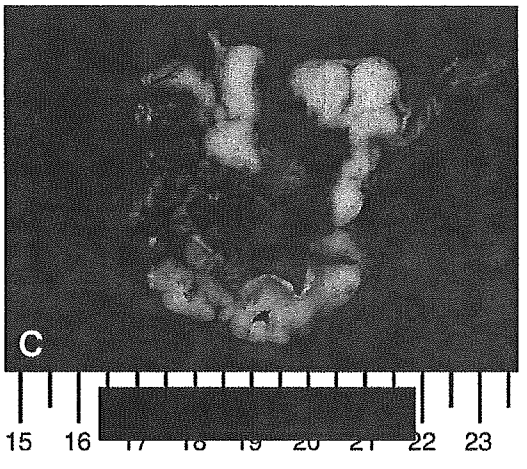

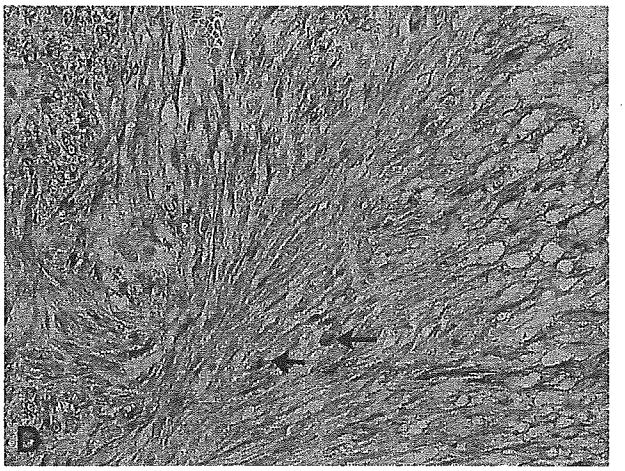

A 53-year-old man with melena and anemia was referred for double-balloon endoscopy (DBE). A previous EGD, colonoscopy, and small-bowel enteroclysis examination revealed no specific findings. Transabdominal US and abdominal CTs were negative. Laboratory tests on admission revealed a Hb level of 6.3 g/dL (normal: 11.3-15.2 g/dL). After transfusion of two units of blood, DBE was performed and revealed an ulcerated and excavated mass, with a diameter of approximately 6 cm, in the proximal ileum (**A**). Gastrografin (Nihon Schering, Osaka, Japan) was infused into the proximal side of the tumor through the DBE, with its distal balloon inflated (*arrow*), blocking the back flow of the contrast to enhance visualization of the segment. Radiography demonstrated an ulcerated mass (**B**). The involved segment of ileum was surgically resected (**C**). Pathologic examination showed that it was a GI stromal tumor (GIST) with a number of mitotic nuclei (*arrows*), which suggests malignancy. Immunohistochemistry showed that the cells were kit positive (**D**; Immunohistochemical stain for c-kit, orig. mag. ×200) but did not express Desmin and S-100.

Michiko Iwamoto, MD, Hironori Yamamoto, MD, Hiroto Kita, MD, Keijiro Sunada, MD, Yoshikazu Hayashi, MD, Hiroyuki Sato, MD, Kentaro Sugano, MD, *Department of Internal Medicine, Division of Gastroenterology, Jichi Medical School, Tochigi, Japan*

PII: S0016-5107(05)01585-3

Commentary

Two recently developed techniques to visualize the entire small bowel are videocapsule enteroscopy (VCE) and double-balloon endoscopy (DBE). VCE is purely diagnostic, whereas DBE also has therapeutic capability. The present case illustrates the use of DBE to provide a roentgen image of a segment of tumor-bearing small bowel and entices us to imagine its therapeutic potential were the lesion to have been removable.

Lawrence J. Brandt, MD
Associate Editor of Focal Points

Contamination with Hepatitis B Virus DNA in Gastrointestinal Endoscope Channels: Risk of Infection on Reuse after On-Site Cleaning

Y. Ishino
K. Ido
K. Sugano

Abstract

Background and Study Aims: The incidence of viral contamination in the air, water and suction/accessory channels of gastrointestinal endoscopes was examined in order to evaluate the risk of infection.

Materials and Methods: After endoscopic examinations, including biopsy procedures, in 17 patients who were positive for hepatitis B virus surface antigen and eight patients who were positive for hepatitis C virus antibody, the endoscopes were cleaned on site by suctioning and flushing the air and water channels with an enzyme detergent. First samples were then collected by flushing 5 ml of sterile water through each channel. After mechanical reprocessing, second samples were collected in the same way. Virological studies were carried out with real-time polymerase chain reactions for hepatitis B virus DNA and hepatitis C virus RNA.

Results: Hepatitis B virus DNA was detected in five of the first samples recovered from the suction/accessory channels of the endoscopes (titers of 1.3×10^4 to 2.5×10^5 copies/ml), while no contamination was detected after reprocessing ($P = 0.0445$). The first samples from one water channel and three air channels were also positive for hepatitis B virus DNA, but were negative after reprocessing ($P > 0.5$, $P = 0.227$, respectively). No hepatitis C virus RNA was detected in any of the samples.

Conclusions: These results indicate that all of the channels were potential sources of viral infection.

Introduction

Endoscopic transmission of infectious agents continues to be a serious problem. Previous studies have drawn attention to deficiencies in endoscope reprocessing procedures, and more effective methods of achieving high-level disinfection have been proposed [1–6]. On the basis of these data, a number of guidelines on endoscope disinfection have been published [7–11], and efforts to revise and improve these guidelines have continued with revisions and improvements as awareness of the risk of transmitting infection through incorrect reprocessing procedures has increased. Although several reports have found that reprocessing procedures following the present guidelines are adequate for high-level disinfection [12,13], reports of nosocomial infection via endoscopic procedures continue to appear, including transmission of hepatitis B virus (HBV) [14,15], hepatitis C virus (HCV) [16], and *Helicobacter pylori* [17,18].

One suggested cause of endoscopic infection is inadequate cleaning procedures, and in particular failure to carry out brush cleaning. The guidelines all emphasize the importance of meticulous cleaning of channels, especially the suction/accessory channel, before disinfection [7–9]. In a previous report, our group demonstrated contamination of both the air and water channels of used upper gastrointestinal endoscopes by measuring residual protein volumes in the lumen and by microbial surveillance [6]. The study emphasized that the air and water channels should be brushed before disinfection. After contact with disinfectants, organic soiling in the channels can form an adhesive substance, which can then harbor infectious agents, and even a single con-

Institution
Dept. of Gastroenterology, Jichi Medical School, Tochigi, Japan

Corresponding Author
Y. Ishino, M.D. · Dept. of Gastroenterology · Jichi Medical School · Minamikawachi-machi · Kawachi Gun · Tochigi 329-0498 · Japan · Fax: +81-285-44-8297 · E-mail: ishino@jichi.ac.jp

Submitted 21 March 2004 · **Accepted after Revision** 10 December 2004

Bibliography
Endoscopy 2005; 37 (6): 548–551 © Georg Thieme Verlag KG Stuttgart · New York · ISSN 0013-726X
DOI 10.1055/s-2005-861316

taminated channel can be a source of infection. In most endoscopes, the only way of cleaning the air and water channels is by flushing them with air and water [7]. Regrettably, the majority of endoscope manufacturers have not changed the complex structure of the air and water channels, which therefore remain inaccessible to brushing. Experimental studies on virally contaminated endoscopes have suggested that the suction/accessory channels were a potential source of viral infection [19,20]. The present study evaluated viral contamination separately for each of the air, water, and suction/accessory channels of endoscopes that had been used to examine patients with HBV and HCV.

Materials and Methods

Following upper gastrointestinal examinations, including biopsy procedures, in patients who were positive for hepatitis B surface antigen (HBsAg) or HCV antibody, the endoscopes used (Pentax EG-2940, Pentax, Tokyo, Japan) were immediately cleaned on site by suctioning 200 ml tap water with a detergent (Cidezyme, Johnson and Johnson, Inc., Sherman, Texas, USA) and then flushing air and water through the air and water channels, respectively, for 2 min. The suction/accessory channel was similarly flushed with an air-filled syringe after water had been suctioned with the detergents. The surface of the insertion tube was wiped three times with wet gauze. After on-site cleaning, samples were taken (first samples) by flushing 5 ml aliquots of sterile water through each suction/accessory, air, and water channel. Residual fluid was purged from the channels with an air-filled syringe. The endoscopes were then washed manually with tap water and the detergent. The endoscopes used in this study have air and water channels wide enough for direct brushing. Each channel was brushed three times with the appropriate brushes (Pentax CS-5021 and CS-3025, Pentax, Tokyo, Japan), and then washed and disinfected by automatic endoscopic reprocessors (Pyser System 83, Custom Ultrasonics, Ivyland, Pennsylvania, USA), with disinfection using 2% glutaraldehyde for 20 min. The reprocessing procedures were carried out in accordance with the guidelines of the Association for Professionals in Infection Control and Epidemiology [7]. After cleaning, samples from the three respective channels were taken again as before (second samples).

Real-time polymerase chain reaction (PCR) was used to detect HBV DNA in samples taken from endoscopes used in HBV patients [21] and HCV RNA in samples from endoscopes used in HCV patients [22]. The incidence of positive findings for HBV DNA or HCV RNA in the endoscopes was compared between the first and second samples for each channel. The results were analyzed using Fisher's exact test.

Results

Seventeen HBsAg-positive patients (Table **1**) underwent endoscopy with biopsy during the study period. The first samples from five suction/accessory endoscope channels were contaminated, while contamination was not observed in any of the second samples from suction/accessory channels. The suction/accessory channel was thus significantly decontaminated by the brushing/automatic endoscopic reprocessor procedure ($P = 0.0445$). The first samples from three air channels and one water channel were also positive for HBV DNA; HBV DNA titers as assessed by PCR for the positive endoscopes are shown in Table **2**. The second samples from the air and water channels showed no contamination ($P = 0.227$, $P > 0.5$, respectively).

Table **1** Data on serum hepatitis B e antigen (HBeAg) and antibody (HBeAb) in patients undergoing endoscopy with the endoscopes studied

Endoscope no.	*HBeAg*	*HBeAb*
1	–	+
2	–	+
3	NE	NE
4	–	+
5	–	+
6	–	+
7	–	+
8	–	+
9	–	+
10	–	+
11	–	+
12	–	+
13	–	+
14	–	+
15	+	+
16	–	+
17	–	+

+: Positive; –: negative; NE: not examined. Endoscope no. 3 was used in a patient with hepatitis B virus liver cirrhosis.

Eight patients who were positive for HCV antibody underwent endoscopy with biopsy during the study period. None of the endoscopes were positive for HCV RNA in either the first or second samples.

Discussion

While detection of viral DNA does not necessarily mean that infective viral particles are present, these results still imply a potential risk of viral transmission via contaminated channels. The present study was a preliminary investigation, although the results show that some air and water channels were still contaminated with HBV DNA after on-site cleaning, as were some suction/accessory channels – so that cleaning by flushing with air and water alone was insufficient to prevent HBV contamination. This is consistent with the findings of a study by Deva et al. [23] in which laparoscopes contaminated with duck hepatitis B virus were investigated. Viral transmission occurred after the instruments were rinsed with water alone. Although laparoscopes are easier to clean, as they do not have internal channels, viral contamination persisted.

Table 2 Titers (copies/ml) of hepatitis B virus DNA on polymerase chain reaction testing in endoscopes that were positive after on-site cleaning

Endoscope no.	Suction/accessory channel	Air channel	Water channel
2	1.1×10^5		
3	2.5×10^5	1.1×10^3	
4	8.8×10^4	4.9×10^2	5.0×10^2
10	1.8×10^4		
12		5.6×10^3	
16	1.3×10^4		

Several studies have documented the contamination of endoscope channels in clinical settings [6,14,24,25]. Vesley et al. investigated the microbial bioburden of each channel of in-use endoscopes [24], and showed that every channel could be contaminated with bacteria after an endoscopic procedure. Birnie et al. reported on the possible transmission of HBV during endoscopy [14]; the authors suspected that the air and water channels were involved in the infection. Reports of HBV endoscopic transmission in Japan have suggested similar findings [15]. Since the air and water channels were probably not cleaned or even flushed with glutaraldehyde, infections occurred. Deva et al. also documented viral contamination of the biopsy/suction channels of endoscopes used in HBV patients [25], and reported that the channels were contaminated with HBV after disinfection without brushing. Also, since patients undergo insufflation during the examination, it is intuitively clear that the resulting positive pressure may contribute to the retrograde movement of fluids from the patient, including blood, up all of the instrument's hollow-bore channels. To our knowledge, this is the first study demonstrating postendoscopic HBV contamination of all channels, including the air and water channels, of upper gastrointestinal endoscopes, even after immediate flushing with water and a detergent.

Chanzy et al. studied the experimental HCV contamination of all gastrointestinal endoscope channels [20] and found that HCV RNA was not detected by PCR after disinfection. The results of the present study also showed that contamination was undetectable in any of the channels after endoscopic examinations in patients who were positive for HCV antibody. There are several possible explanations for these findings. Firstly, as HCV RNA is relatively fragile, it may be damaged during the sampling procedure. Secondly, sample titers may be below detectable levels; HCV RNA might have been detected if the brushing and flushing solutions had been combined [26]. Alternatively, on-site cleaning may have been sufficient to wash out the virus completely.

The reprocessing of endoscopes is a serious issue requiring international attention. Although guidelines for endoscope reprocessing have been formulated by endoscopic societies all over the world, endoscopic transmission of infectious agents still occurs – mostly due to failure to comply with the recommended guidelines, and in particular a lack of brushing [27]. In an Italian national survey, only 69.7% of the endoscopic units used brushing to clean the biopsy/suction channels [28]. Cheung et al. analyzed reprocessing procedures in the United States [29] and found that suctioning detergent through the biopsy channels, followed by brushing of the channels and valves, was carried out by 90.7% of the respondents. In Japan, a questionnaire survey showed that only two-thirds of the respondents observed the guidelines [30]. In a case of HCV transmission via colonoscopy, the biopsy/suction channel was reused without being cleaned with a brush [16]. On-site cleaning merely assists the subsequent washing and disinfection procedure and does not achieve disinfection on its own. As the present study shows, all three channels may remain contaminated with pathogens such as viruses after on-site cleaning. Reusing endoscopes after on-site cleaning alone can therefore be hazardous and should be avoided.

The samples were taken after on-site cleaning and after automatic reprocessing with meticulous brushing. Samples were not collected after brushing. The results do not show that brushing alone or automatic reprocessing alone was effective. The guidelines recommend an endoscopic reprocessing procedure involving meticulous brushing and automatic reprocessing. The present findings suggest that the recommended procedure is effective.

Several guidelines have noted that the major problem with infection control in relation to endoscope reprocessing is the instruments' design [7–9]. There have been relatively few improvements in the design to facilitate thorough cleaning and disinfection. Reports have pointed out the risk of infection due to the complicated design of endoscope channels [6,19,20]. Pentax is the only manufacturer to have developed new products with brushable channels. These products have been available for several years, but other manufacturers have not yet followed suit. The findings of the present study underline the importance of cleaning the air and water channels by brushing. It would be desirable for all endoscope manufacturers to make the air and water channels accessible for brush cleaning.

Conclusions

The reprocessing of endoscopes should involve every channel, including the air and water channels, as all of the channels are potential sources of contamination after use. Manufacturers should develop endoscopes that have improved access to all occluded areas and allow verifiably effective cleaning.

Acknowledgment

We are grateful to the staff of the Endoscopic Examination Center at Jichi Medical School for their assistance.

References

[1] Lynch DA, Porter C, Murphy L et al. Evaluation of four commercial automatic endoscope washing machines. Endoscopy 1992; 24: 766–770
[2] Ido K, Ishino Y, Ota Y et al. Deficiencies of automatic endoscopic reprocessors: a method to achieve high-grade disinfection of endoscopes. Gastrointest Endosc 1996; 44: 583–586

[3] Urayama S, Kozarek RA, Sumida S et al. Mycobacteria and glutaraldehyde: is high-level disinfection of endoscopes possible? Gastrointest Endosc 1996; 43: 451–456
[4] Tremain SC, Orientale E, Rodney WM. Cleaning, disinfection, and sterilization of gastrointestinal endoscopes: approaches in the office. J Fam Pract 1991; 32: 300–305
[5] Fraser VJ, Zuckerman G, Clouse RE et al. A prospective randomized trial comparing manual and automated endoscope disinfection methods. Infect Control Hosp Epidemiol 1993; 14: 383–389
[6] Ishino Y, Ido K, Koiwai H et al. Pitfalls in endoscope reprocessing: brushing of air and water channels is mandatory for high-level disinfection. Gastrointest Endosc 2001; 53: 165–168
[7] Alvarado CJ, Reichelderfer M. APIC guideline for infection prevention and control in flexible endoscopy. Association for Professionals in Infection Control. Am J Infect Control 2000; 28: 138–155
[8] Ogoshi K, Akamatsu T, Iishi H et al. JGES guideline for cleaning and disinfection in gastrointestinal endoscopy. Dig Endosc 2000; 12: 369–382
[9] Systchenko R, Marchetti B, Canard JN et al. Guidelines of the French Society of Digestive Endoscopy: recommendations for setting up cleaning and disinfection procedures in gastrointestinal endoscopy. Endoscopy 2000; 32: 807–818
[10] BSG EndoscopyCommittee Working Party. Cleaning and disinfection of equipment for gastrointestinal endoscopy: report of a working party of the British Society of Gastroenterology endoscopy committee. Gut 1998; 42: 585–593
[11] Rey J, Kruse A, Axon T et al. ESGE guidelines for the prevention of endoscopic transmission of type C hepatitis and update on Creutzfeldt–Jakob disease. Endoscopy 1997; 29: 203–204
[12] Kovacs BJ, Chen YK, Kettering JD et al. High-level disinfection of gastrointestinal endoscopes: are current guidelines adequate? Am J Gastroenterol 1999; 94: 1546–1550
[13] Foliente RL, Kovacs BJ, Aprecio RM et al. Efficacy of high-level disinfectants for reprocessing GI endoscopes in simulated-use testing. Gastrointest Endosc 2001; 53: 456–462
[14] Birnie GG, Quigley EM, Clements GB et al. Endoscopic transmission of hepatitis B virus. Gut 1983; 24: 171–174
[15] Kasugai T, Yoshii Y, Shikata J et al. Digestive endoscopy and HBV infection (first report) [in Japanese with English abstract]. Gastroenterol Endosc 1984; 27: 2727–2733
[16] Bronowicki JP, Venard V, Botté C et al. Patient-to-patient transmission of hepatitis C virus during colonoscopy. N Engl J Med 1997; 337: 237–240
[17] Tytgat GN. Endoscopic transmission of Helicobacter pylori. Aliment Pharmacol Ther, 1995; 9 (Suppl 2): 105–110
[18] Akamatsu T, Tabata K, Hironga M et al. Transmission of *Helicobacter pylori* infection via flexible fiberoptic endoscopy. Am J Infect Control 1996; 24: 396–401
[19] Bond WW, Moncada RE. Viral hepatitis B infection risk in flexible fiberoptic endoscopy. Gastrointest Endosc 1978; 24: 225–230
[20] Chanzy B, Duc-Bin DL, Rousset B et al. Effectiveness of a manual disinfection procedure in eliminating hepatitis C virus from experimentally contaminated endoscopes. Gastrointest Endosc 1999; 50: 147–151
[21] Abe A, Inoue K, Tanaka T et al. Quantitation of hepatitis B virus genomic DNA by real-time detection PCR. J Clin Microbiol 1999; 37: 2899–2903
[22] Takeuchi T, Katsume A, Tanaka T et al. Real-time detection system for quantification of hepatitis C virus genome. Gastroenterology 1999; 116: 636–642
[23] Deva AK, Vickery K, Zou J et al. Establishment of an in-use testing method for evaluating disinfection of surgical instruments using the duck hepatitis B model. J Hosp Infect 1996; 33: 119–130
[24] Vesley D, Melson J, Stanley P. Microbial bioburden in endoscope reprocessing and an in-use evaluation of the high-level disinfection capabilities of Cidex PA. Gastroenterol Nurs 1999; 22: 63–68
[25] Deva AK, Vickery K, Zou J et al. Detection of persistent vegetative bacteria and amplified viral nucleic acid from in-use testing of gastrointestinal endoscopes. J Hosp Infect 1998; 39: 149–157
[26] Alfa MJ, Jackson M. A new hydrogen peroxide-based medical-device detergent with germicidal properties: comparison with enzymatic cleaners. Am J Infect Control 2001; 29: 168–177
[27] Di Marino AJJ. Noncompliance with FDA and society guidelines for endoscopic reprocessing: implications for patient care. Gastrointest Endosc Clin N Am 2000; 10: 283–294
[28] Orsi GB, Filocamo A, di Stefano L et al. Italian national survey of digestive endoscopy disinfection procedures. Endoscopy 1997; 29: 732–740
[29] Cheung RJ, Ortiz D, Di Marino AJJ. GI endoscopic reprocessing practices in the United States. Gastrointest Endosc 1999; 50: 362–368
[30] Cleaning and Disinfection Committee for Endoscopes, Japanese Gastroenterological Endoscopy Society. The Cleaning and Disinfection Committee for Endoscopes of the Japanese Gastroenterological Endoscopy Society report: questionnaire survey of digestive endoscopy disinfection procedure [in Japanese]. Gastroenterol Endosc 1999; 41: 215–219

Experimental trial for diagnosis of pancreatic ductal carcinoma based on gene expression profiles of pancreatic ductal cells

Madoka Ishikawa,[1] Koji Yoshida,[2] Yoshihiro Yamashita,[1] Jun Ota,[1,3] Shuji Takada,[1] Hiroyuki Kisanuki,[1] Koji Koinuma,[1] Young Lim Choi,[1] Ruri Kaneda,[1] Toshiyasu Iwao,[4] Kiichi Tamada,[5] Kentaro Sugano[5] and Hiroyuki Mano[1,3,6]

[1]Division of Functional Genomics, Jichi Medical School, 3311-1 Yakushiji, Kawachi-gun, Tochigi 329-0498; [2]Department of Medicine, Kawasaki Medical School, Okayama 701-0192; [3]CREST, Japan Science and Technology Agency, 4-1-8, Honcho, Kawaguchi-shi, Saitama 332-0012; [4]Gastroenterological Center, Aizu Central Hospital, 1-1 Tsuruga-machi, Aizu-Wakamatsu, Fukushima 956-8611; and [5]Division of Gastroenterology, Jichi Medical School, 3311-1 Yakushiji, Kawachi-machi, Kawachi, Tochigi 329-0498, Japan

(Received November 18, 2004/Revised April 25, 2005/Accepted April 27, 2005/Online Publication July 22, 2005)

Pancreatic ductal carcinoma (PDC) remains one of the most intractable human malignancies, mainly because of the lack of sensitive detection methods. Although gene expression profiling by DNA microarray analysis is a promising tool for the development of such detection systems, a simple comparison of pancreatic tissues may yield misleading data that reflect only differences in cellular composition. To directly compare PDC cells with normal pancreatic ductal cells, we purified MUC1-positive epithelial cells from the pancreatic juices of 25 individuals with a normal pancreas and 24 patients with PDC. The gene expression profiles of these 49 specimens were determined with DNA microarrays containing >44 000 probe sets. Application of both Welch's analysis of variance and effect size-based selection to the expression data resulted in the identification of 21 probe sets corresponding to 20 genes whose expression was highly associated with clinical diagnosis. Furthermore, correspondence analysis and 3-D projection with these probe sets resulted in separation of the transcriptomes of pancreatic ductal cells into distinct but overlapping spaces corresponding to the two clinical classes. To establish an accurate transcriptome-based diagnosis system for PDC, we applied supervised class prediction algorithms to our large data set. With the expression profiles of only five predictor genes, the weighted vote method diagnosed the class of samples with an accuracy of 81.6%. Microarray analysis with purified pancreatic ductal cells has thus provided a basis for the development of a sensitive method for the detection of PDC. (*Cancer Sci* 2005; 96: 387–393)

Pancreatic ductal carcinoma (PDC), arising from the pancreatic ductal cells, accounts for more than 85% of all pancreatic malignancies, and is one of the most intractable malignancies in humans.[1,2] Effective therapy for PDC is hampered by the lack of specific clinical symptoms, with a 5-year survival rate of only 20 to 30%. An increase in the serum concentration of the protein CA19-9 is a reliable marker for PDC, but such an increase is only apparent in the advanced stages of disease.[3] Furthermore, although activating mutations of the *KRAS* oncogene have been detected in PDC cells, such mutations are also associated with other conditions, including chronic pancreatitis.[4,5]

DNA microarray analysis allows the simultaneous monitoring of the expression level of thousands of genes[6,7] and is therefore a potentially suitable approach for the identification of novel molecular markers for detection of the early stages of PDC. However, caution is warranted in simple comparisons between normal and cancerous pancreatic tissues. Because normal pancreatic tissue is composed mostly of exocrine and endocrine cells, and cancerous pancreatic tissue consists mostly of tumor cells that arise from ductal epithelial cells, a simple comparison between these two tissues tends to identify cell lineage-dependent gene expression differences.[8]

To minimize such misleading data that are attributable to population-shift effects, we have set up a depository for pancreatic ductal cells purified from pancreatic juice collected from patients during endoscopic retrograde cholangiopancreatography (ERCP). Comparison of such pancreatic ductal cell preparations between control individuals and PDC patients by DNA microarray analysis has the potential to identify specific gene markers for the latter. Indeed, an initial screening of a limited number of samples (from three individuals with a normal pancreas and six with PDC) with a DNA microarray of 3456 genes yielded candidates for new PDC marker genes.[8]

We have now expanded this project by using a larger number of specimens: 25 from individuals with a normal pancreas and 24 from PDC patients. Each purified preparation of pancreatic ductal cells was subjected to microarray experiments with Affymetrix HGU133 A&B GeneChips, which contain >44 000 probe sets corresponding to ~33 000 human genes. The application of sophisticated bioinformatics techniques to this large data set (a total of 2 156 000 data points) resulted in the establishment of an algorithm to differentiate transformed ductal cells from normal ones.

Materials and Methods

Preparation of pancreatic ductal cells. The study subjects comprised individuals who underwent ERCP and collection of pancreatic juice for cytological examination. The subjects gave informed consent and the study was approved by the institutional review board of Jichi Medical School. Diagnosis of patients was confirmed on the basis of the combination of results obtained by ERCP, cytological examination of pancreatic juice, abdominal computed tomography, and measurement of the serum concentration of CA19-9, as well as of follow-up observations. Approximately one-third of each specimen of pancreatic juice was used to purify $MUC1^+$ ductal cells.[9]

Cells were collected from the pancreatic juice by centrifugation and were resuspended in 1 mL of MACS binding buffer (150 mM NaCl, 20 mM sodium phosphate [pH 7.4], 3% fetal bovine serum, 2 mM ethylenediamine tetraacetic acid). They were then incubated for 30 min at 4°C with 0.5 μg of a mouse

[6]To whom correspondence should be addressed. E-mail: hmano@jichi.ac.jp

Abbreviations: ACTB, β-actin; EPPK1, epiplakin 1; ERCP, endoscopic retrograde cholangiopancreatography; H2BFB, H2B histone family, member B; KNN, *k* nearest neighbor; NRCAM, neuronal cell adhesion molecule; PCR, polymerase chain reaction; PDC, pancreatic ductal carcinoma; PLOD2, procollagen-lysine, 2-oxoglutarate 5-dioxygenase 2; RASAL2, RAS protein activator-like 2; SCGB3A1, secretoglobin, family 3A, member 1; SST, somatostatin; WV, weighted vote.

 doi:10.1111/j.1349-7006.2005.00064.x

monoclonal antibody to MUC1 (Novocastra Laboratories, Newcastle upon Tyne, UK), washed with MACS binding buffer, and mixed with MACS MicroBeads conjugated with antibodies to mouse immunoglobulin G (Miltenyi Biotec, Auburn, CA, USA). The resulting mixture was subjected to chromatography on a miniMACS magnetic cell separation column (Miltenyi Biotec), and the eluted $MUC1^+$ cells were divided into portions and stored at −80°C. Portions of the unfractionated cells as well as the isolated $MUC1^+$ cells of each individual were stained with Wright–Giemsa solution to examine the purity of the ductal cell-enriched fractions.

Microarray experiments. Total RNA was extracted from the $MUC1^+$ cell preparations with the use of an RNeasy Mini column and RNase-free DNase (Qiagen, Valencia, CA, USA) and was subjected to two rounds of mRNA amplification with T7 RNA polymerase.[10] The high fidelity of the amplification step has been demonstrated previously.[11] One microgram of the amplified cRNA was then converted to double-stranded cDNA by PowerScript reverse transcriptase (BD Biosciences Clontech, Palo Alto, CA, USA), and the cDNA was used to prepare biotin-labeled cRNA with an ENZO BioArray Transcript Labeling Kit (Affymetrix, Santa Clara, CA, USA). Hybridization of the labeled cRNA with GeneChip HGU133 A&B microarrays, which contain >44 000 probe sets, was performed with the GeneChip system (Affymetrix). The mean expression intensity of the internal positive control probe sets[12] was set to 500 arbitrary units (U) in each hybridization, and the fluorescence intensity of each test gene was normalized accordingly. All normalized array data are available at the Gene Expression Omnibus web site (http://www.ncbi.nlm.nih.gov/geo) under the accession number GSE1542.

Statistical analysis. Hierarchical clustering of the data set, Welch's analysis of variance (ANOVA), and k nearest neighbor (KNN) method-based class prediction were performed with GeneSpring 6.2 software (Silicon Genetics, Redwood, CA). The weighted vote (WV) method[13] was performed with GeneCluster 2.1.7.[14] Correspondence analysis[15] for all genes showing a significant difference in expression was performed by using ViSta software.[16] Each sample was plotted in three dimensions based on the coordinates obtained from the correspondence analysis. With the exception of the effect-size selection, in which linear values were used for calculation, all normalized expression values were transformed to logarithms prior to analyses.

Real-time PCR analysis. Portions of nonamplified cDNA were subjected to PCR with a QuantiTect SYBR Green PCR Kit (Qiagen). The amplification protocol comprised incubations at 94°C for 15 s, 57°C for 30 s, and 72°C for 60 s. Incorporation of the SYBR Green dye into PCR products was monitored in real time with an ABI PRISM 7900 HT sequence detection system (PE Applied Biosystems, Foster City, CA, USA), thereby allowing determination of the threshold cycle (C_T) at which exponential amplification of products begins. The C_T values for cDNA corresponding to the β-actin gene (*ACTB*) and to the target genes were used to calculate the abundance of target gene mRNA relative to that of *ACTB* mRNA. The oligonucleotide primers for PCR were as follows: 5′-CCATCATGAAGTGTGACGTGG-3′ and 5′-GTCCGCCTAGAAGCATTTGCG-3′ for *ACTB*, 5′-CCCGTGAACCACCTCATAG-3′ and 5′-AGCGTCTTGTCCTCAGGTGTA-3′ for the secretoglobin, family 3A, member 1 gene (*SCGB3A1*), and 5′-GATGAAATGAGGCTTGAGCTG-3′ and 5′-GTTTCTAATGCAAGGGTCTCG-3′ for the somatostatin gene (*SST*).

Results

Transcriptome of pancreatic ductal cells. As demonstrated previously, affinity purification with antibodies to MUC1 yielded an apparently homogeneous preparation of pancreatic ductal cells.[8] With this approach, we purified pancreatic ductal cell specimens from 25 individuals with a normal pancreas and 24 patients with PDC. Clinical characteristics for the latter individuals are summarized in Table 1. All 49 specimens were each subjected to DNA microarray analysis with Affymetrix HGU133 A&B GeneChips, which contain >44 000 probe sets.

Table 1. Clinical characteristics of patients with PDC

Patient	Age (years)	Sex	Cytological examination	Atypical cell proportion*	Clinical stage†
ID073	74	Male	V	H	IVa
ID086	72	Female	IV	M	IVa
ID088	65	Male	V	L	IVb
ID089	70	Female	III	L	III
ID090	72	Male	III	L	IVa
ID095	85	Female	III	L	0
ID096	76	Female	IV	L	IVa
ID098	61	Female	IV	L	IVa
ID103	65	Male	V	H	IVb
ID117	76	Female	IV	L	IVa
ID119	73	Female	V	L	IVa
ID120	70	Female	III	M	0
ID125	75	Male	II	L	I
ID131	67	Female	II	L	IVa
ID142	69	Male	III	H	I
ID147	51	Male	V	L	IVb
ID202	56	Female	III	M	IVa
ID203	73	Male	III	M	I
ID218	51	Male	III	L	0
ID224	71	Male	V	L	IVa
ID225	50	Female	III	L	IVa
ID227	65	Male	I	L	III
ID229	60	Female	IV	M	IVa
ID234	71	Male	III	L	IVa

*Isolated ductal cells contained <20% (L), 20–40% (M) or ≧ 40% (H) of atypical cells. †Clinical stage was determined according to the proposal of Isaji *et al.*[25]

For analysis of the gene expression data, we first set the condition that the expression level of a given probe set should receive the 'Present call' (from Microarray Suite 5.0 software) in at least 30% (n = 15) of the samples in order to exclude transcriptionally silent genes from the analysis. A total of 7778 probe sets fulfilled this selection criterion. Unsupervised two-way hierarchical clustering analysis[17] was then applied to the 49 specimens based on the expression profiles of these 7778 probe sets, generating a dendrogram in which the samples are clustered according to the similarity in expression pattern of the probe sets (Fig. 1). Although this dendrogram contained a large branch consisting mostly of PDC patients, normal and cancer specimens did not form separate, diagnosis-dependent branches. The transcriptome of virtually all expressed genes thus did not differ sufficiently between normal and cancerous ductal cells to allow diagnosis.

PDC-specific molecular signature. To capture a PDC-specific molecular signature, we next identified genes whose expression level differed significantly between the normal and cancerous ductal cells. Application of Welch's ANOVA ($P < 0.001$) for this purpose yielded 26 out of the 7778 probe sets examined. However, some of the probe sets thus identified had low absolute expression levels throughout the samples, even though the ratio of the expression levels between the two classes was relatively large. To eliminate such 'nearly silent' genes and to enrich genes whose expression level was markedly increased in at least one of the classes, we further selected those whose effect size (absolute difference in mean expression intensities)[18] between the two classes was ≧ 50 U.

 doi:10.1111/j.1349-7006.2005.00064.x

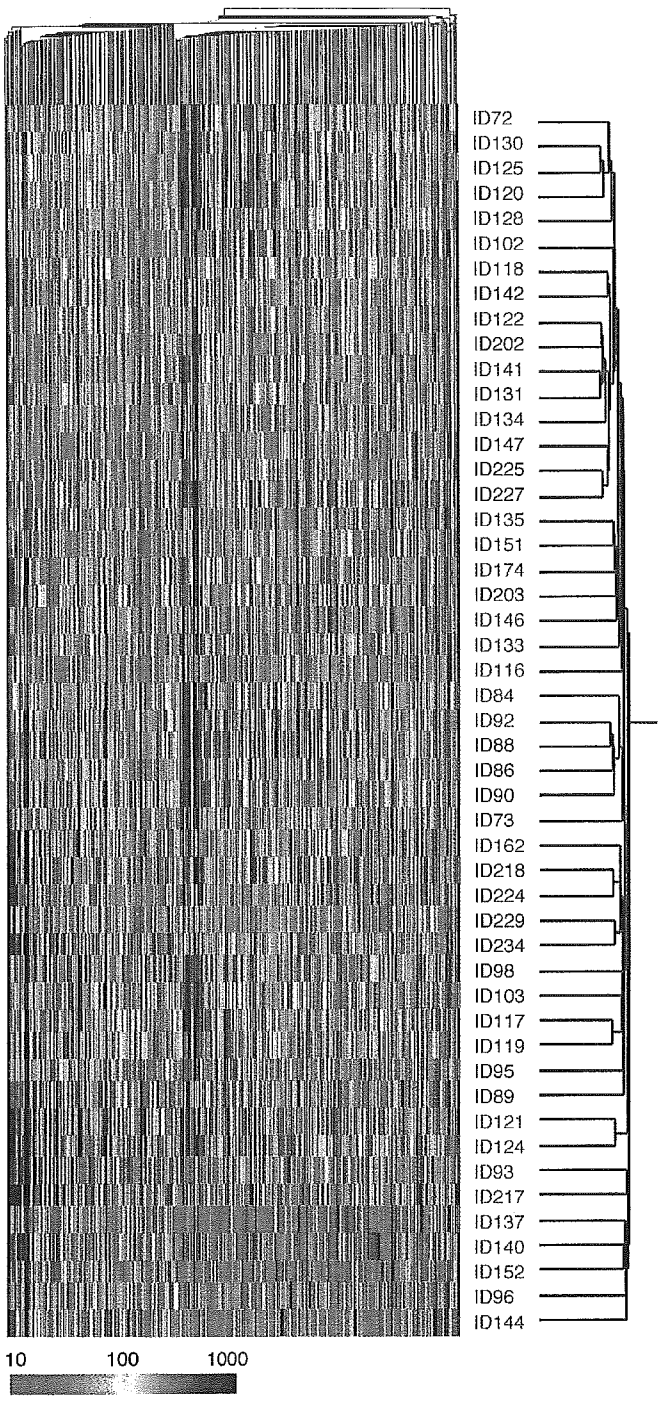

Fig. 1. Gene expression profiles of the purified pancreatic ductal cells. Hierarchical two-way clustering of the study subjects (normal ductal cell specimens [green] and PDC specimens [red]) was performed on the basis of the expression profiles of 7778 probe sets. Each column corresponds to a single probe set, and each row corresponds to a separate subject. The expression level of probe sets is color-coded according to the indicated scale.

With this approach, we identified 21 probe sets (corresponding to 20 independent genes) whose expression levels differed significantly between the two clinical conditions. Construction of a dendrogram for the expression profiles of these 21 probe sets revealed that the subjects were grouped into two major branches (Fig. 2a). Although each branch corresponded approximately to the two clinical classes, a few subjects were still misclassified in both branches. It was not clear, however, whether this failure to clearly separate the two clinical classes was due to an inadequacy of the separation power of the clustering method or to the heterogeneity of the samples within each clinical class. Furthermore, these results did not address whether normal and cancerous ductal cells are truly distinct from each other from the point of view of gene expression profiles.

To address these issues, we attempted to visualize the similarity or difference between the two classes. Correspondence analysis is a relatively new approach to the decomposition of multidimensional data.[15] It allows not only a low-dimensional projection of expression profiles for numerous genes, but also measurement both of the contribution of each gene to a given extracted dimension and of the contribution of each extracted dimension to the total complexity. Correspondence analysis of the expression data of the 21 probe sets shown in Fig. 2a reduced the number of dimensions from 21 to three. On the basis of the calculated 3-D coordinates for each sample, the specimens were then projected into a virtual space (Fig. 2b). Although most of the normal samples were positioned in a region of the space distant from that occupied by the PDC specimens, the two groups were not separated completely. Decomposition of the data set was thus not sufficiently effective to achieve a high accuracy in differential diagnosis.

Supervised class prediction. We next attempted class prediction by using two supervised algorithms. The WV method was recently developed to assign binary classes based on gene expression profiles.[13] A defined number of 'class predictor' genes whose expression contrasts the two classes most effectively are first selected in a training data set. A weighting factor, which reflects how well a gene is correlated with the class distinction, is also calculated for each gene. The expression levels of the class predictors are then quantitated in the test data set, and the 'prediction strength' is determined on the basis of the expression intensities and weighting factors of the predictors. The WV method has been successfully used to differentiate acute myeloid leukemia from acute lymphoid leukemia,[13] as well as diffuse large B cell lymphoma with poor prognosis from that with good prognosis.[19]

The KNN method, like the WV method, first involves the selection of a defined number of predictor genes. It then finds nearest neighbors to the classes based on a distance function for pairs of observations. The KNN method predicts the class of a given test sample based on the majority of votes among the nearest neighbors.[20]

To measure precisely the class prediction ability of these two methods, we performed a cross-validation trial for each with our data set: One sample was therefore set aside and the program was trained with the remaining 48 samples; the class of the withheld test sample was then predicted by the program, and the trial was repeated for each of the 49 samples to calculate the overall accuracy of the program.

For both WV and KNN methods, the cross-validation was performed with the 49 specimens and with different numbers of class predictor genes (n = 1 to 20, 30, 40, 50, 60, 70, 80, 90, or 100). Both methods had similar error rates, with the WV method having a slightly lower error rate than the KNN method (Fig. 3a). The best prediction accuracy (81.6%) was obtained by the WV method with five class predictor genes. In this cross-validation, different sets of five predictors were selected for each leave-one-out trial, with a total of 11 probe sets (corresponding to 10 genes) used as predictors. Two-way clustering of the expression profiles of these 11 probe sets yielded the dendrogram shown in Fig. 3b. It should be noted that two probe sets (DKFZp564I1922 and EPPK1) were selected as the predictors in all 49 leave-one-out trials.

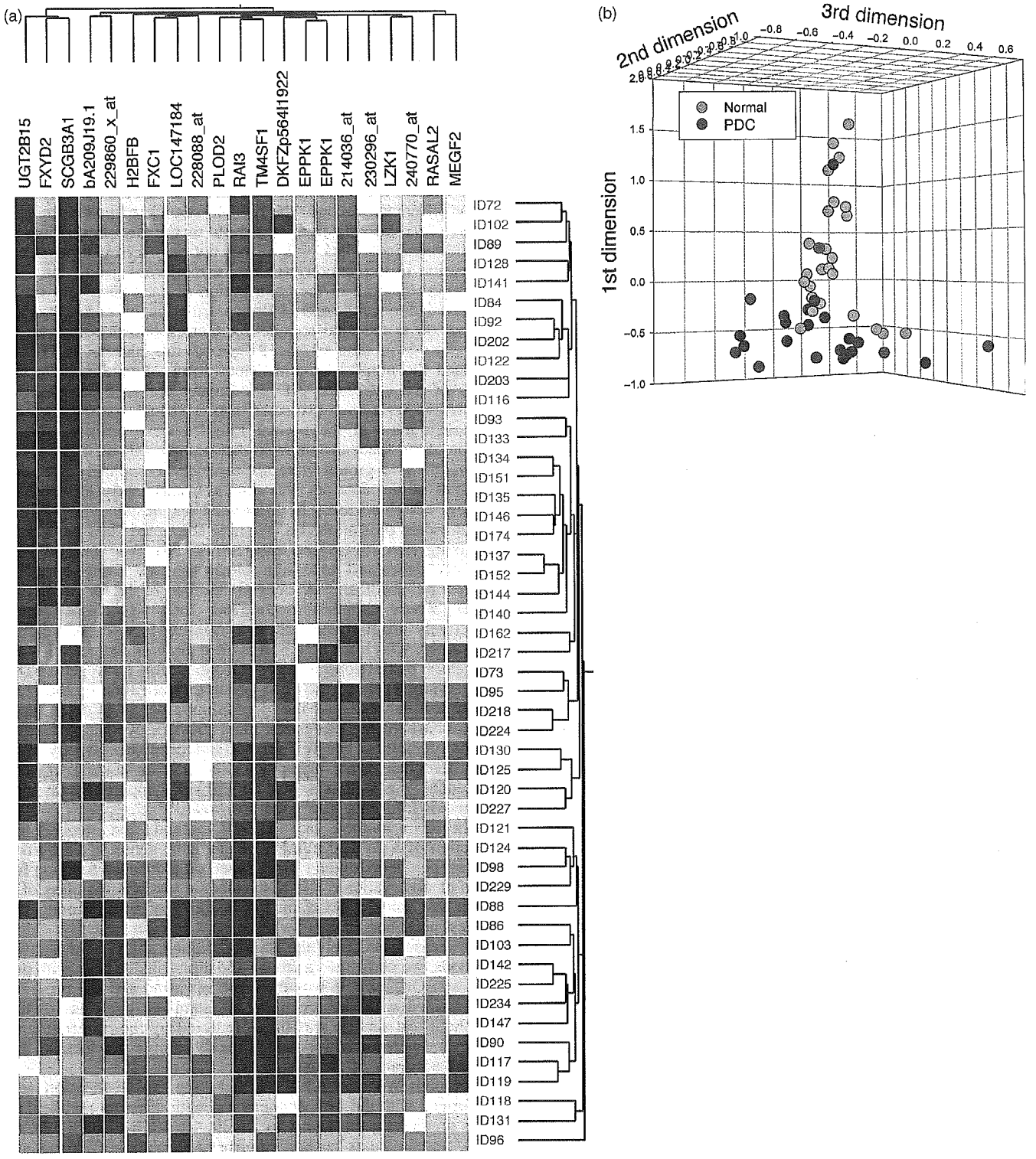

Fig. 2. Isolation of a PDC-specific molecular signature. (a) Dendrogram of the 21 probe sets whose expression level differed significantly (Welch's ANOVA, $P < 0.001$) with an effect size of ≧ 50 U between normal and cancerous specimens. Each row corresponds to a separate subject, and each column to a probe set whose expression is color-coded according to the scale in 1. Gene symbols are shown at the top; 229860_x_at, 228088_at, 214036_at, 230296_at, and 240770_at are expressed sequence tag IDs designated by Affymetrix. Detailed information on the genes and their expression levels is provided in Supplementary Information at the *Cancer Science* web site. (b) Correspondence analysis of the 21 probe sets identified three major dimensions in their expression profiles. Projection of the specimens into a virtual space with these three dimensions revealed that those from individuals with a normal pancreas and those from patients with PDC were partially separated.

 doi:10.1111/j.1349-7006.2005.00064.x

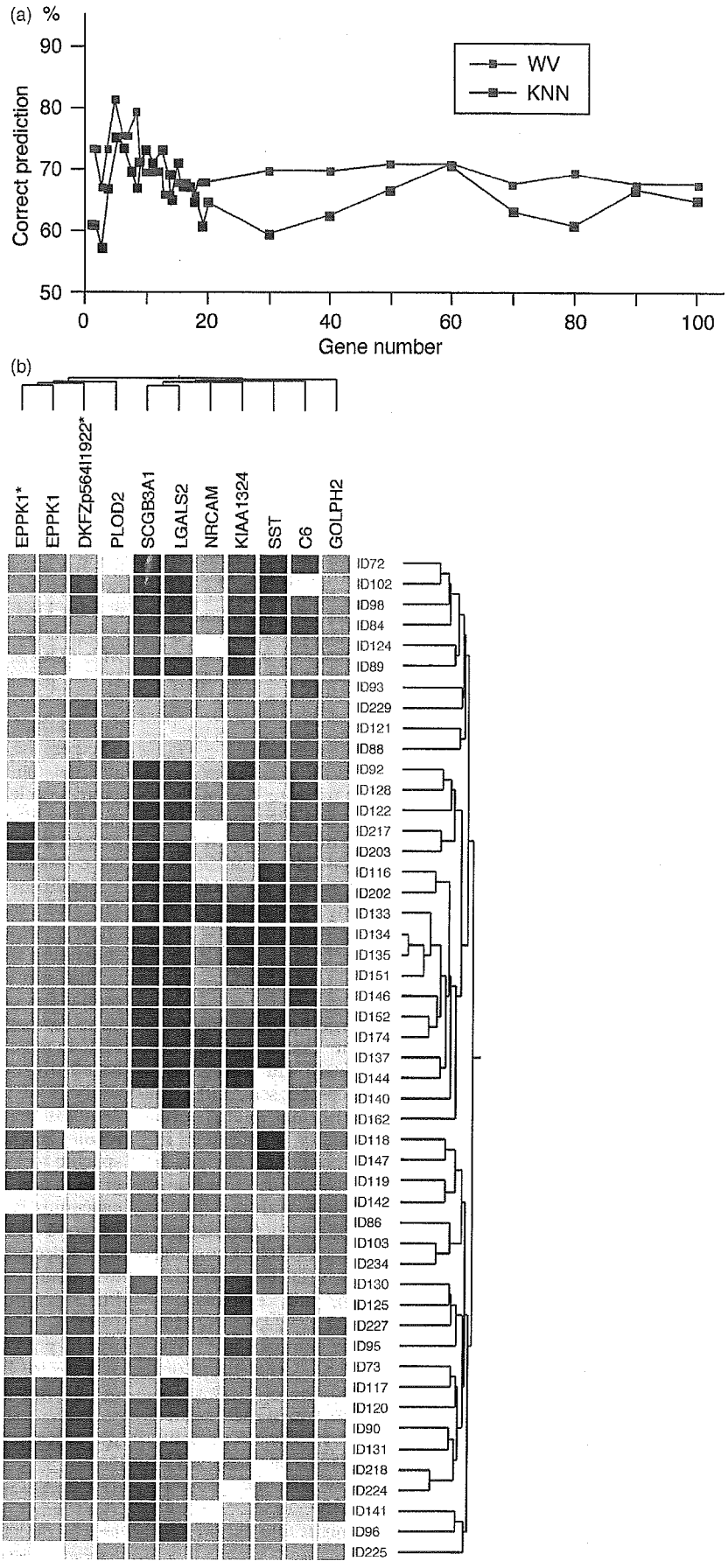

Fig. 3. Supervised class prediction. (a) Cross-validation trials for class prediction of normal or PDC specimens based on various numbers of predictor genes were performed with the WV or KNN methods. Correct prediction rate (%) is plotted for each trial. (b) Expression profiles of 11 probe sets identified by the WV method with five predictors. Samples are clustered according to the similarity in the expression pattern of the 11 probe sets. Asterisks indicate the two probe sets selected in all trials. Detailed information on the genes and their expression levels is provided in Supplementary Information at the *Cancer Science* web site.

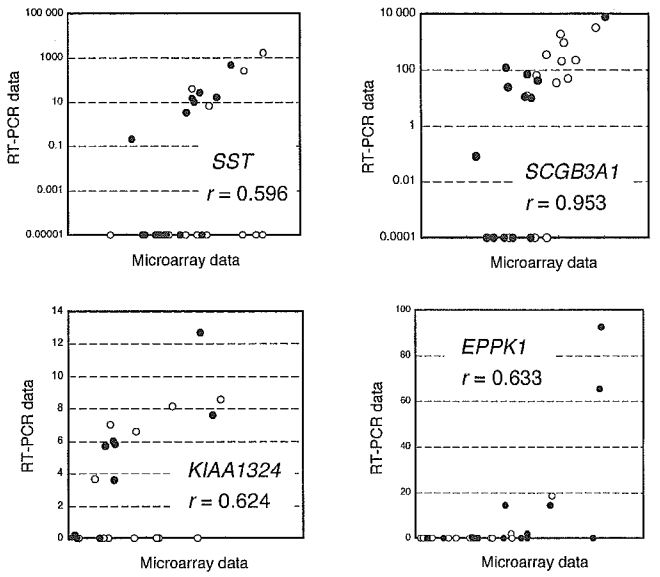

Fig. 4. Validation by reverse transcription and real-time PCR analysis of gene expression profiles obtained by microarray analysis. The relative amounts of mRNA corresponding to *SST, SCGB3A1, KIAA1324* or *EPPK1* in the MUC1$^+$ cells derived from (○) healthy individuals or (●) patients with PDC were determined by reverse transcription and real-time PCR with *ACTB* transcripts as the internal standard. The resulting values are plotted against those obtained by microarray analysis. Pearson's correlation coefficient (*r*) values are provided for each comparison.

Confirmation of expression data. To confirm the gene expression profiles obtained by microarray analysis, we measured the mRNA levels of some genes by reverse transcription and quantitative real-time PCR analysis. The relative amounts of mRNA derived from the *SST* (GenBank accession number NM_001048) or *SCGB3A1* (GenBank accession number AA742697) genes, for example, determined by this latter approach were highly correlated with those quantitated by microarray analysis (Fig. 4).

Discussion

In the present study, we constructed the largest gene expression database available to date for pancreatic ductal cells. Our statistical approach to identify genes associated with a diagnosis of PDC resulted in the extraction of 21 probe sets, three of which were preferentially expressed in normal ductal cells and the remaining 18 were preferentially expressed in cancerous ductal cells. The latter group contained the genes for H2B histone family member B (*H2BFB*; GenBank accession number BC002842), RAS protein activator-like 2 (*RASAL2*; GenBank accession number NM_004841), procollagen-lysine, 2-oxoglutarate 5-dioxygenase 2 (*PLOD2*; GenBank accession number NM_000935), adlican (DKFZp564I1922; GenBank accession number AF245505), and epiplakin 1 (*EPPK1*; GenBank accession number AL137725). H2BFB functions as a linker histone in nucleosome compaction.[21] The increased expression of *H2BFB* in PDC cells therefore probably reflects the increased proliferation rate of these cells. RASAL2 shares a GTPase-activating protein (GAP)-related domain with members of the RAS-GAP family of proteins and is thought to contribute to the regulation of small GTP-binding proteins. *RASAL2* is localized within the prostate cancer susceptibility locus at chromosome 1q25[22], so an altered activity of the encoded protein might thus be directly linked to carcinogenesis.

The expression profile of these disease-associated genes was not, however, sufficient to separate the specimens into the normal or cancer class with a high accuracy. We therefore applied sophisticated algorithms in the supervised mode in an attempt to achieve this goal. In our trials of the WV and KNN methods with various numbers of predictor genes, the WV method trained with five genes gave the best result. The accuracy of correct diagnosis achieved (81.6%) is higher than that obtained by cytological examination of pancreatic juice.[23]

In the 'leave-one-out' trials for all 49 samples, a total of 11 probe sets were chosen by the WV algorithm as the class predictors. These probe sets corresponded to 10 genes, including those for EPPK1, DKFZp564I1922, PLOD2, SCGB3A1, SST, and neuronal cell adhesion molecule (*NRCAM*; GenBank accession number NM_005010). NRCAM belongs to the immunoglobulin (Ig) superfamily of proteins, contains multiple repeats of the Ig domain in its extracellular region, and is expressed at the surface of neuronal cells. The DKFZp564I1922 protein also contains 12 repeats of the Ig domain.[24] Increased expression of these Ig domain-containing proteins may thus be a specific property and a novel molecular marker of PDC.

Among the 10 genes used in the WV analysis, only two (those for EPPK1 and DKFZp564I1922) were chosen as predictors in all 49 trials. In addition, the Welch's ANOVA strategy and the WV method selected five probe sets in common, including two sets for EPPK1, one for SCGB3A1, one for PLOD2, and one for DKFZp564I1922.

Cytological examination revealed that, among the individuals with PDC in our study, 16 patients had <20% of atypical cells in the purified ductal cell specimens ('L' in Table 1), three patients had ≧ 40% of such cells ('H'), and the other five patients had 20–40% of such cells ('M'). We thus examined whether the proportion of atypical cells in the specimens affected the expression intensities of the selected genes. The expression levels of the genes in Fig. 2a was, for instance, compared by Student's *t*-test between the individuals in the L and M groups, and between those in the M and H groups. Surprisingly, none of the genes in Fig. 2a were differentially expressed in a significant manner between these groups (data not shown). Therefore, our microarray-based prediction scheme should be of clinical importance even for patients with pancreatic juice containing small amounts of cancer cells.

Our strategy to identify a PDC-specific gene expression profile for purified pancreatic ductal cells should provide the basis for several possible scenarios for the early detection of PDC in the clinical setting. One scenario would be a microarray-based diagnosis of PDC with a sophisticated algorithm for analysis of the expression of a limited number of genes (as demonstrated in the present study). A second scenario would require an extension of our project to isolate single gene markers specific to PDC; the expression of such genes should be negligible in non-cancerous cells but would be markedly increased in cancerous cells. Such PDC-specific single gene markers would be good candidates for the construction of a sensitive PCR-based detection system for PDC. A third scenario may involve the identification of soluble proteins among the products of PDC-specific genes that could be detected in the serum of patients. Further expansion of our gene expression database would probably facilitate the development of such detection systems for PDC, which would improve the long-term prognosis of individuals with this intractable disease.

Acknowledgments

This work was supported in part by a Grant-in-Aid for research on the Third Term Comprehensive Control Research for Cancer from the Ministry of Health, Labour, and Welfare of Japan, and by a grant from the Research Foundation for Community Medicine.

 doi:10.1111/j.1349-7006.2005.00064.x

References

1 Bomman PC, Beckingham IJ. Pancreatic tumours. *Br Med J* 2001; **322**: 721–3.
2 Rosewicz S, Wiedenmann B. Pancreatic carcinoma. *Lancet* 1997; **349**: 485–9.
3 Sawabu N, Watanabe H, Yamaguchi Y, Ohtsubo K, Motoo Y. Serum tumor markers and molecular biological diagnosis in pancreatic cancer. *Pancreas* 2004; **28**: 263–7.
4 Kondo H, Sugano K, Fukayama N *et al.* Detection of point mutations in the K-ras oncogene at codon 12 in pure pancreatic juice for diagnosis of pancreatic carcinoma. *Cancer* 1994; **73**: 1589–94.
5 Furuya N, Kawa S, Akamatsu T, Furihata K. Long-term follow-up of patients with chronic pancreatitis and K-ras gene mutation detected in pancreatic juice. *Gastroenterology* 1997; **113**: 593–8.
6 Schena M, Shalon D, Davis RW, Brown PO. Quantitative monitoring of gene expression patterns with a complementary DNA microarray. *Science* 1995; **270**: 467–70.
7 Duggan DJ, Bittner M, Chen Y, Meltzer P, Trent JM. Expression profiling using cDNA microarrays. *Nat Genet* 1999; **21**: 10–4.
8 Yoshida K, Ueno S, Iwao T *et al.* Screening of genes specifically activated in the pancreatic juice ductal cells from the patients with pancreatic ductal carcinoma. *Cancer Sci* 2003; **94**: 263–70.
9 Terada T, Ohta T, Sasaki M, Nakamura Y, Kim YS. Expression of MUC apomucins in normal pancreas and pancreatic tumours. *J Pathol* 1996; **180**: 160–5.
10 Van Gelder RN, von Zastrow ME, Yool A, Dement WC, Barchas JD, Eberwine JH. Amplified RNA synthesized from limited quantities of heterogeneous cDNA. *Proc Natl Acad Sci USA* 1990; **87**: 1663–7.
11 Oshima Y, Ueda M, Yamashita Y *et al.* DNA microarray analysis of hematopoietic stem cell-like fractions from individuals with the M2 subtype of acute myeloid leukemia. *Leukemia* 2003; **17**: 1990–7.
12 Affymetrix [web site on the Internet]. Support: Mask files. Available from URL: http://www.affymetrix.com/support/technical/mask_files.affx
13 Golub TR, Slonim DK, Tamayo P *et al.* Molecular classification of cancer: class discovery and class prediction by gene expression monitoring. *Science* 1999; **286**: 531–7.
14 Broad Institute [web site on the Internet]. GeneCluster 2.0. Available from URL: http://www.broad.mit.edu/cancer/software/genecluster2/gc2.html
15 Fellenberg K, Hauser NC, Brors B, Neutzner A, Hoheisel JD, Vingron M. Correspondence analysis applied to microarray data. *Proc Natl Acad Sci USA* 2001; **98**: 10781–6.
16 ViSta. [web site on the Internet]. ViSta: the visual statistics system. Available from URL: http://www.visualstats.org
17 Alon U, Barkai N, Notterman DA *et al.* Broad patterns of gene expression revealed by clustering analysis of tumor and normal colon tissues probed by oligonucleotide arrays. *Proc Natl Acad Sci USA* 1999; **96**: 6745–50.
18 Dhanasekaran SM, Barrette TR, Ghosh D *et al.* Delineation of prognostic biomarkers in prostate cancer. *Nature* 2001; **412**: 822–6.
19 Shipp MA, Ross KN, Tamayo P *et al.* Diffuse large B-cell lymphoma outcome prediction by gene-expression profiling and supervised machine learning. *Nat Med* 2002; **8**: 68–74.
20 Dudoit S, Fridlyand J, Speed TP. [pre-print PDF on the Internet]. Comparison of discrimination methods for the classification of tumors using gene expression data. Available from URL: http://www.stat.berkeley.edu/tech-reports/index.html
21 Albig W, Kardalinou E, Drabent B, Zimmer A, Doenecke D. Isolation and characterization of two human H1 histone genes within clusters of core histone genes. *Genomics* 1991; **10**: 940–8.
22 Noto S, Maeda T, Hattori S, Inazawa J, Imamura M, Asaka M, Hatakeyama M. A novel human RasGAP-like gene that maps within the prostate cancer susceptibility locus at chromosome 1q25. *FEBS Lett* 1998; **441**: 127–31.
23 Nakaizumi A, Tatsuta M, Uehara H *et al.* Cytologic examination of pure pancreatic juice in the diagnosis of pancreatic carcinoma. The endoscopic retrograde intraductal catheter aspiration cytologic technique. *Cancer* 1992; **70**: 2610–4.
24 Strausberg RL, Feingold EA, Grouse LH *et al.* Generation and initial analysis of more than 15 000 full-length human and mouse cDNA sequences. *Proc Natl Acad Sci USA* 2002; **99**: 16 899–903.
25 Isaji S, Kawarada Y, Umemoto S. Classification of pancreatic cancer. Comparison of Japanese and UICC classifications. *Pancreas* 2004; **28**: 231–4.

Supplementary Material

The following supplementary material is available for this article online:

Table S1. Annotation information and expression intensity data for the genes shown in Figure 2A.

Table S2. Annotation information and expression intensity data for the genes shown in Figure 3B.

日消誌　2005；102：1412—1416

原　著

カロリーメイト缶®を用いた胆　収縮能超音波検査

新井由　玉田喜一　佐藤幸浩
和田伸　田野茂夫　花塚和伸
大橋　菅野健太郎[1)]

要旨：胆嚢収縮能超音波検査において一般に用　うれている卵黄に代わりカロリーメイト缶®を用い，そ
の有用性について検討した．健常人ボランティ　27名を対象とし，腹部超音波検査にて空腹時胆嚢容
積をellipsoid法にて求めた．カロリーメイト缶　欠用後，30分後と60分後に胆嚢容積を測定し，胆嚢
収縮率（EF）を求めた．空腹時胆嚢容積は平均　3.5m*l*，EFは平均で30分後53%，60分後62%
と充分な胆嚢収縮が見られ，カロリーメイト缶　胆嚢収縮剤として有用と考えられた．また，空腹時胆
嚢容積が4m*l*に満たない例では前日の脂肪食　響を除くために，禁食を厳重にして再検する必要が
あると考えられた．

索引用語：胆嚢機能評価，胆嚢収縮率，超音波，カ　リーメイト®，Ellipsoid法

はじめに

近年，腹部エコーの普及により無症状胆嚢結石が発見される頻度が増加している．これらの患者において経過観察または経口溶解療法，体外衝撃波砕石術などの適応を判断するため，安全かつ無痛のない胆嚢機能評価法が重要となる．また，胆嚢機能異常は胆嚢コレステロール結石[1)]，胆嚢炎[2)]，胆嚢腺筋腫症[3)]，糖尿病[4)5)]，慢性膵炎[6)]などの各疾患との関連が報告されており，簡便な胆嚢機能評価法が普及すれば，これらの疾患の患者の大規模な評価が可能になる．

今日，胆嚢機能評価には超音波[7)8)]，排泄性胆嚢造影，CT[9)]などにて胆嚢容積を検討する方法などが開発されている．胆嚢収縮剤として従来使用されていたCeruletide，Secretinが相次いで製造中止となり，現在胆嚢収縮能超音波検査においては一般に卵黄2個が用いられている[10)]が，煩雑であるとともにサルモネラ菌や鳥インフルエンザ感染の危険など衛生面の問題も生じている．Cacao drinkがCeruletide同様胆嚢収縮剤として有用であったとの報告もあり[11)]，今回，われわれは卵黄に代わり安全かつ簡便なカロリーメイト缶®を用い，その有用性について検討した．

I 目　的

カロリーメイト缶®摂取前後の胆嚢容積を測定し，カロリーメイト缶®が卵黄の代わりに胆嚢収縮剤として用いることができるかを検討する．

II 方　法

腹部超音波検査実習時に被検者を志願してくれた医学生または研修医のボランティア27名を対象とした．大豆および牛乳のアレルギー歴を問診し，本検査の意味を説明して口頭で承諾を得た．男性16人，女性11人で，年齢は平均23歳（22～26歳）であった．約12時間の絶食後，空腹時腹部超音波検査にて胆嚢容積をellipsoid法[7)]にて求めた（Figure 1）．卵黄2個を用いた場合60分後[8)]，cacao drink[11)]，クリニミール®[12)]を用いた場合30分後に胆嚢は最大収縮を示したことから，同程度の時間で最大収縮が得られると考え，簡便のため測定時間はカロリーメイト缶®200m*l*（Table 1）飲用後30分（n＝27），60分（n＝18）とし，胆嚢容積を求めた．胆嚢容積は，いずれも複数回測定し

1）自治医科大学消化器内科

Table 1. カロリーメイト缶®と卵黄2個の比較

	カロリーメイト缶® (200m*l*)	卵黄2個
エネルギー (kcal)	200	131
脂質 (g)	4.4	11
タンパク質 (g)	4.4～7	5.5

Table 2. 男女間の比較

	全体	男性	女性	男女間のp値
体重 (kg)	59 ± 12	66 ± 10	48 ± 4.5	0.0003
空腹時胆嚢容積 (m*l*)	13.5 ± 8.3	16.7 ± 8.9	8.9 ± 5.5	0.016
EF30 (%)	53 ± 19	57.4 ± 36	44.8 ± 36	0.38
EF60 (%)	62 ± 24	28.6 ± 94	54 ± 49	0.52

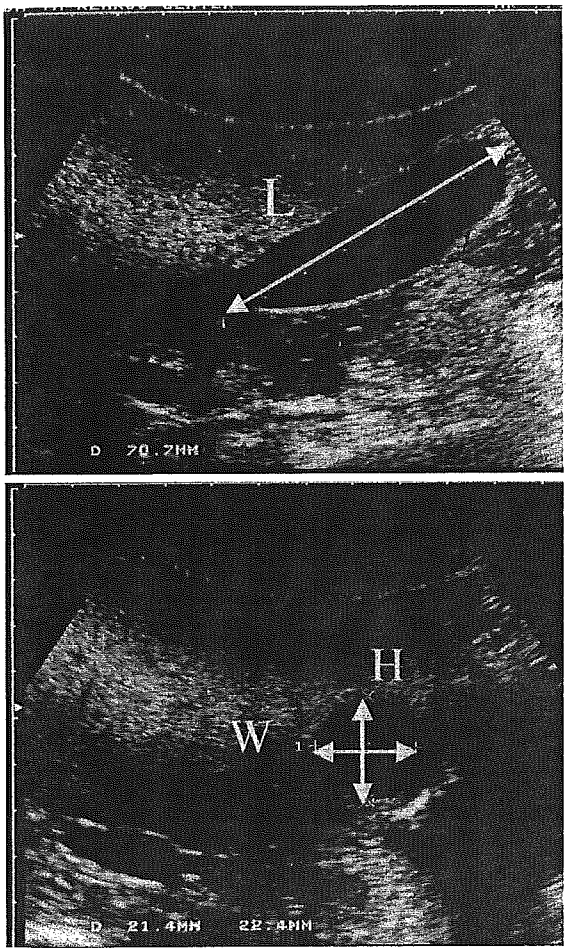

Figure 1. ellipsoid法による胆嚢容積算出：胆嚢容積 (m*l*) =0.52×L×W×H.
EF (%) = (空腹時胆嚢容積－内服後胆嚢容積) ÷空腹時胆嚢容積×100

平均胆嚢容積を用いた．カロリーメイト缶®には植物性油脂が使用されており，その多くが長鎖脂肪酸であり，不飽和脂肪酸は約80%である．カロリーメイト缶®飲用前後の胆嚢容積から胆嚢収縮率 (Ejection Fraction，以下EF) を次式で求め，検討した．

EF(%) = {(空腹時胆嚢容積－内服後胆嚢容積) ÷空腹時胆嚢容積} ×100

有意差についてはpairedまたは分散分析後にunpaired t-testを，相関はPearsonの相関係数を用いて検定し，$p<0.05$ を有意差ありと判定した．

III 結　果

空腹時胆嚢容積は13.5±8.3m*l*，男性16.7±8.6m*l*，女性8.9±5.2m*l* であり，体重とともに男女間で有意差が見られた．30分後EF(以下EF30)，60分後EF (以下EF60) は負の値となった2名を除くと53±19%，62±24% であり，男女間で有意差はなかった (Table 2)．

体重と空腹時胆嚢容積は相関があり (Figure 2)，EF30，EF60とは相関がなかった ($p=0.22$, $p=0.84$)．EFが負となったのは空腹時胆嚢容積が2.7m*l*，3.1m*l* と最小の2名であり，空腹時胆嚢容積が4m*l* 未満の3名とそれ以上の24名ではEF30，EF60ともに有意差が見られた(Figure 3)．2名でEF60がEF30を下回ったほかは，EF60はEF30に比べ横ばいもしくは軽度上昇傾向であったが，有意差はなかった．被検者それぞれの

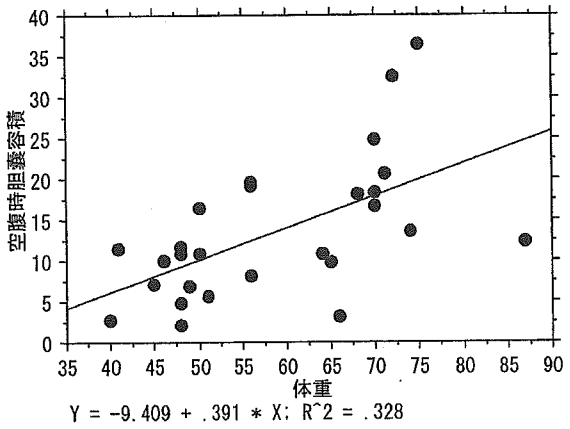

Figure 2. 体重と空腹時胆嚢容積：体重と空腹時胆嚢容積は p＝0.001，相関係数 0.57 にて相関を認める．図の下部に回帰直線の関数式と決定係数を示す．

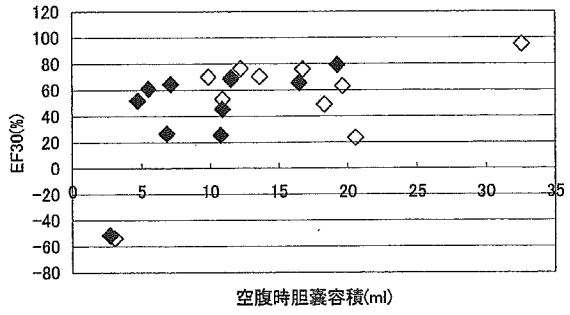

Figure 3. 空腹時胆嚢容積と EF30：◇男性，◆女性，空腹時胆嚢容積が 4m*l* 未満の 3 名とそれ以上の 24 名では EF30，EF60 ともに有意差が見られた（ともに p＝＜0.0001）．

EF30 と EF60 には相関係数 0.81 と強い相関が認められた（Figure 4）．

Ⅳ 考　察

卵黄 2 個を用いた胆嚢収縮能超音波検査（ellipsoid 法）での空腹時胆嚢容積は平均 10.3m*l*[13]から 24m*l*[8]，EF30 は 48%，EF60 は 70%[8]との報告がある．今回われわれの検討では空腹時胆嚢容積は平均 13.5m*l* であり，既報と同様であった．空腹時胆嚢容積は体重と相関があった．男女間で有意差が見られたが，体重差の影響が考えられる（Table 2, Figure 2）．若い女性では胆嚢の変形が強い傾向があり，ellipsoid 法では胆嚢を規則正しい形と仮定して計算しているため，胆嚢容積が過小評価された可能性もある．

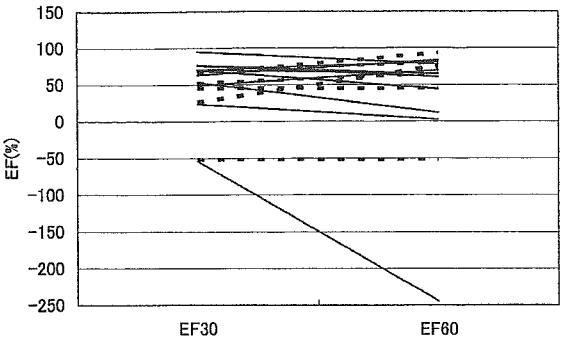

Figure 4. EF30 と EF60 の被検者個々の変化：—男性，---女性，EF30 と EF60 は有意差なく（p＝0.57），被検者それぞれの EF30 と EF60 には相関係数 0.81 と強い相関が認められた（p＜0.0001）．

カロリーメイト缶®200m*l* の脂質含有量は 4.4g であり，M サイズの卵黄 2 個平均 11g[14]に比べると少ない（Table 1）．しかし，300kcal としたクリニミール®（脂質 9.39g）とエレンタール®（脂質 0.54g）の両者でコレシストキニンの有意上昇，胆嚢の有意収縮が報告されており[15]，今回われわれが用いたカロリーメイト缶®にても同様の傾向が見られると予測できる．カロリーメイト缶®を用いた EF30 は平均 53%，EF60 は平均 62% と卵黄を用いた場合に遜色のない胆嚢収縮が見られた．一方，卵黄を用いた報告では EF60 が EF30 に比べ大きく上昇したのに対し，今回の検討では両者の間に有意差が見られなかった（Figure 4）．十二指腸チューブから卵黄を注入した場合，血漿コレシストキニンは 10 分後から有意に上昇，30 分後に頂値 42pmol/*l* となり，胆嚢は 40 分後に最大収縮を示したとの報告[12]があるが，経口投与ではより遅れると考えられる．同一著者によるクリニミール®（400kcal，脂質 12.5g）を経口投与した報告では，血漿コレシストキニンは 5 分後から有意に上昇，20 分後に頂値 23.3pmol/*l* となり，胆嚢は 30 分後に最大収縮を示したと報告している．今回われわれが用いたカロリーメイト缶®もクリニミール®同様に液体であり卵黄摂取に比べ十二指腸への流出および吸収が早いためにコレシストキニンが早く頂値となり胆嚢の最大収縮が早く得られる

と考えられる．カロリーメイト缶®負荷ではEF30とEF60には強い相関があり，両者に有意差がないことから，EF30の良好な症例ではEF60の計測を省略することが可能と思われ，検査はより簡便となると考えられた．

EFが負となったのは空腹時胆嚢容積が最小の2名であり，両者とも前日の夕食に高脂肪食を摂取していた．うち1名では12時間の絶食後であるにもかかわらずエコー上胃内容物が観察された．この被検者において検査前日の夕食を脂質7g程度の低脂肪食として14時間の絶食後に再検したところ，空腹時胆嚢容積12.8m*l*，30分後EF 16.7%，60分後EF 53.3%となった．このように同一症例内での変動[13]の影響は大きく，1回の検査のみで胆嚢収縮能不良とは判断できない．この被検者において，60分後EFは平均と差がないが，30分後EFが低値であるのは胃排泄遅延が影響した可能性がある．空腹時胆嚢容積が小さい例では前日の高脂肪食が影響した可能性があり，再検の必要がある．われわれの検討においては空腹時胆嚢容積が4m*l*未満とそれ以上ではEFに有意差が生じており，禁食を厳重にして再検する必要があると考えられたが，症例数が少ないため更なる検討が必要である．

胃排泄遅延のような消化吸収機能障害の他にEFに影響を与えるものとして，糖尿病患者，胆嚢結石患者，乳頭機能障害などが考えられる．糖尿病患者，胆嚢結石患者では空腹時胆嚢容積の増加，EFの減少が報告されている[5)16)17)]．また糖尿病患者では卵黄摂取によるコレシストキニンの上昇にもかかわらず収縮能が低下しており，神経障害がその要因として大きいと考えられている[17)]．胆道疾患や上記のように胆嚢機能に影響を及ぼす疾患においても，今後本法を用いて検討し報告したい．

結　語

カロリーメイト缶®は胆嚢収縮能超音波検査において卵黄に代わる胆嚢収縮剤として有用であった．30分後にEF高値であれば60分後の計測を省き胆嚢収縮能良好と判断でき，検査はより簡便となると考えられた．

本研究の主旨は2004年5月15日第279回日本消化器病学会関東支部例会にて発表した．

文　献

1) Marzio L, Innocenti P, Genovesi N, et al : Role of oral cholecystography, real-time ultrasound, and CT in evaluation of gallstones and gallbladder function. Gastrointest Radiol 17 ; 257-261 : 1992
2) Pozo MJ, Camello PJ, Mawe GM : Chemical mediators of gallbladder dysmotility. Curr Med Chem 11 ; 1801-1812 : 2004
3) 高石　修，小林絢三：胆嚢Adenomyomatosisと胆道Dyskinesiaとの関連．胆と膵17；455-458：1996
4) Meguro T, Shimosegawa T, Satoh A, et al : Gallbladder emptying and cholecystokinin and pancreatic polypeptide responses to a liquid meal in patients with diabetes mellitus. J Gastroenterol 32 ; 628-634 : 1997
5) Guliter S, Yilmaz S, Karakan T : Evaluation of gallbladder volume and motility in non-insulin-dependent diabetes mellitus patients using real-time ultrasonography. J Clin Gastroenterol 37 ; 288-291 : 2003
6) Mizushima T, Ochi K, Seno T, et al : Gastrobiliary dysmotility in patients with chronic pancreatitis as assessed by a single noninvasive test. Acta Med Okayama 52 ; 55-61 : 1998
7) Dodds WJ, Groh WJ, Darweesh RM, et al : sonographic measurement of gallbladder volume. AJR Am J Roentgenol 145 ; 1009-1011 : 1985
8) 橋本千樹，後藤秀実，廣岡芳樹，他：三次元超音波装置を使用した胆嚢容積，収縮能の検討．胆と膵　20；229-233：1999
9) 花栗勝郎，木村英明，茅嶋恭代，他：Helical-3D-CT-Cholangiographyによる Volume測定法を用いた胆嚢収縮能の評価．日本災害医学会会誌　45；270-278：1997
10) 島田　章，中井吉英：胆道ジスキネジーの超音波学的検討 Caerulein法と卵黄法．超音波医学　18；63-70：1991
11) Nitsche R, Hinrichsen H, Herzig KH, et al : Evaluation of a cacao drink as a simple oral stimulus to assess gallbladder contraction. Z Gastroenterol 36 ; 135-141 : 1998
12) 井上一知，渕上　哲，角昭一郎，他：胆道機能異常の臨床—消化管ホルモン特にCCKの動態から．胆と膵　8；693-700：1987
13) Donald JJ, Fache JS, Buckley AR, et al : Gallbladder contractility : variation in nomal subjects. AJR Am J Roentgenol 157 ; 753-756 : 1991
14) 香川　綾：四訂日本食品標準成分表．四訂食品成分表，女子栄養大学出版部，東京，192-193, 1997

15) 田代充生，秋山俊治，芳川一郎，他：経腸栄養剤が内因性コレシストキニン（CCK）分泌，胃排出および胆嚢収縮に及ぼす影響．Therapeutic Research 24；417-418：2003
16) Sugiyama M, Atomi Y：Does endoscopic papillary balloon dilation affect gallbladder motility? Gastrointest Endosc 50；74-78：1999
17) Mitsukawa T, Takemura J, Ohgo S, et al：Gallbladder function and plasma cholecystokinin levels in diabetes mellitus. Am J Gastroenterol 85；981-985：1990

〔論文受領，平成16年9月8日
受理，平成17年5月25日〕

Ultrasonography with liquid type Calo

Mate® for gallbladder motility

Yuki ARAI, Kichi TAMADA, Yukihiro SAT
Kazunobu HANATSUKA, Akira OHASHI a
. Shinichi WADA, Shigeo TANO,
Kentarou SUGANO[1)]
[1)]*Department of Gastroenterology, Jichi Medical School H*
al

We usually use yolks to assess gallbladder mo
type CalorieMate® as a simple oral stimulus i
sonography before, 30 min after, and 60min aft
the ejection fraction were measured by ellipsoid
tion fraction, and 60-min one were 13.5m*l*, 53%, a
vious reports by yolks. If the fasting volume is lo
fast to reduce the influence of the dinner the day
useful stimulus to assess gallbladder motility.
y by ultrasonography. In this study, we evaluated liquid
ad of yolks. The volunteers (n = 27) underwent ultra-
king liquid type CalorieMate®. Gallbladder volume and
thod. The mean fasting gallbladder volume, 30-min ejec-
52%, respectively. These results were similar to the pre-
than 4m*l*, they should take re-examination after longer
ore the exam. In conclusion, liquid type CalorieMate® is

Key words : Gallbladder, Motility, Ultrasonogra
CalorieMate®, Ellipsoid method

tapraid4/zh0-acel/zh0-acel/zh000406/zh04793d06g | tillotsj | S=5 | 1/7/06 | 2:24 | MS: C-00465-2005 | Ini: 04/PK/BEW | Input-dms

Am J Physiol Cell Physiol 290: C000–C000, 2006.
First published December 21, 2005; doi:10.1152/ajpcell.00465.2005.

Autocrine loop between TGF-β_1 and IL-1β through Smad3- and ERK-dependent pathways in rat pancreatic stellate cells

AQ: 1

Hiroyoshi Aoki,[1] Hirohide Ohnishi,[1] Kouji Hama,[1] Takako Ishijima,[1] Yukihiro Satoh,[1] Kazunobu Hanatsuka,[1] Akira Ohashi,[1] Shinichi Wada,[1] Tomohiko Miyata,[1] Hiroto Kita,[1] Hironori Yamamoto,[1] Hiroyuki Osawa,[1] Kiichi Sato,[1] Kiichi Tamada,[1] Hiroshi Yasuda,[2] Hirosato Mashima,[3] and Kentaro Sugano[1]

[1]*Department of Gastroenterology, Jichi Medical School, Tochigi;* [2]*Division of Gastroenterology, Showa University Fujigaoka Hospital, Kanagawa; and* [3]*Department of Gastroenterology, University of Tokyo School of Medicine, Tokyo, Japan*

Submitted 19 September 2005; accepted in final form 16 November 2005

Aoki, Hiroyoshi, Hirohide Ohnishi, Kouji Hama, Takako Ishijima, Yukihiro Satoh, Kazunobu Hanatsuka, Akira Ohashi, Shinichi Wada, Tomohiko Miyata, Hiroto Kita, Hironori Yamamoto, Hiroyuki Osawa, Kiichi Sato, Kiichi Tamada, Hiroshi Yasuda, Hirosato Mashima, and Kentaro Sugano. Autocrine loop between TGF-β_1 and IL-1β through Smad3- and ERK-dependent pathways in rat pancreatic stellate cells. *Am J Physiol Cell Physiol* 290: C000–C000, 2006. First published December 21, 2005; doi:10.1152/ajpcell.00465.2005.—Pancreatic stellate cells (PSCs) are activated during pancreatitis and promote pancreatic fibrosis by producing and secreting ECMs such as collagen and fibronectin. IL-1β has been assumed to participate in pancreatic fibrosis by activating PSCs. Activated PSCs secrete various cytokines that regulate PSC function. In this study, we have examined IL-1β secretion from culture-activated PSCs as well as its regulatory mechanism. RT-PCR and ELISA have demonstrated that PSCs express IL-1β mRNA and secrete IL-1β peptide. Inhibition of TGF-β_1 activity secreted from PSCs by TGF-β_1-neutralizing antibody attenuated IL-1β secretion from PSCs. Exogenous TGF-β_1 increased IL-1β expression and secretion by PSCs in a dose-dependent manner. Adenovirus-mediated expression of dominant-negative (dn)Smad2/3 expression reduced both basal and TGF-β_1-stimulated IL-1β expression and secretion by PSCs. Coexpression of Smad3 with dnSmad2/3 restored IL-1β expression and secretion by PSCs, which were attenuated by dnSmad2/3 expression. In contrast, coexpression of Smad2 with dnSmad2/3 did not alter them. Furthermore, inhibition of IL-1β activity secreted from PSCs by IL-1β-neutralizing antibody attenuated TGF-β_1 secretion from PSCs. Exogenous IL-1β enhanced TGF-β_1 expression and secretion by PSCs. IL-1β activated ERK, and PD-98059, a MEK1 inhibitor, blocked IL-1β enhancement of TGF-β_1 expression and secretion by PSCs. We propose that an autocrine loop exists between TGF-β_1 and IL-1β in activated PSCs through Smad3- and ERK-dependent pathways.

pancreatic fibrosis; cytokine; chronic pancreatitis

PANCREATIC STELLATE CELLS (PSCs) were recently identified, isolated, and characterized (4, 6). In the normal pancreas, PSCs possess fat droplets containing vitamin A, are quiescent, and can be defined by desmin-positive but α-smooth muscle actin (α-SMA)-negative staining (4). When cultured in vitro, PSCs are autoactivated (autotransformed) and change their morphological and functional features (6). PSCs commence losing vitamin A-containing lipid droplets, highly proliferating, increasing expression of α-SMA, and producing and secreting ECM components such as collagen and fibronectin. Namely, PSCs are autotransformed to myofibroblast-like cells. In vivo PSCs are also activated during both human and experimental pancreatic fibrosis (13). Therefore, PSCs are thought to play an important role in pancreatic fibrogenesis.

TGF-β_1 is one of the major profibrogenic cytokines in various tissues. Recently, TGF-β_1 has been implicated in the etiology of pancreatic fibrosis. It activates PSCs and promotes pancreatic fibrosis (5, 15). TGF-β_1 intracellular signaling is mediated and modulated primarily by the mothers against decapentaplegic homolog (*Drosophila*)-related proteins (Smads) (14, 18). Upon TGF-β_1 binding to the TGF-β type II receptor, the type II receptor kinase phosphorylates the TGF-β type I receptor, leading to activation of the type I receptor. The activated type I receptor kinase phosphorylates Smad homologs 2 and 3 (Smad2/3). Phosphorylated Smad2/3 forms oligomeric complexes with Smad4, and the complexes then translocate into the nucleus. These complexes subsequently activate the transcription of target genes. Thus dual Smad2/3-dependent pathways exist in TGF-β_1 intracellular signaling. Until recently, however, the distinction between Smad2- and Smad3-dependent pathways has been uncertain because of the lack of a methodology to assess their respective roles. Smad2 and Smad3 compete for both the TGF-β receptor and Smad4 binding during their activation; thus their overexpression blocks endogenous Smad3 and Smad2 functions. Therefore, the possibility remains that the effects of Smad2 and Smad3 overexpression on cell functions result from competitive inhibition rather than from enhanced Smad2 and Smad3 activity due to their overexpression. To exclude this possibility, we developed a novel method to analyze the independent roles of Smad2 and Smad3 in TGF-β_1 signal transduction by coexpressing dominant-negative (dn)Smad2/3 with either Smad2 or Smad3 (25). The dnSmad2/3 mutant was generated by substituting Glu for Asp407 of *smad3*, which renders *smad3* defective in TGF-β receptor-dependent phosphorylation. Nevertheless, this mutant possesses a dominant-negative effect on both Smad2 and Smad3 (12). The expression of dnSmad2/3 blocks both endogenous Smad2 and Smad3 functions at the TGF-β receptor-dependent phosphorylation step. Coexpression of either Smad2 or Smad3 with dnSmad2/3 rescues only the Smad2- or Smad3-dependent pathway, respectively, permitting the separation of the Smad2- and Smad3-specific signaling pathways (25).

AQ: 2 AQ: 3 AQ: 4 AQ: 5

AQ: 13 Address for reprint requests and other correspondence: H. Ohnishi, Dept. of Gastroenterology, Jichi Medical School, 3311-1 Yakushiji, Minamikawachi-cho, Kawachi-gun, Tochigi 329-0498, Japan (e-mail: hohnishi@jichi.ac.jp).

The costs of publication of this article were defrayed in part by the payment of page charges. The article must therefore be hereby marked "*advertisement*" in accordance with 18 U.S.C. Section 1734 solely to indicate this fact.

AQ: 13

tapraid4/zh0-acel/zh0-acel/zh000406/zh04793d06g | tillotsj | S=5 | 1/7/06 | 2:24 | MS: C-00465-2005 | Ini: 04/PK/BEW | Input-dms

IL-1β is a potent proinflammatory cytokine and is known to play major roles in the progression of acute pancreatitis leading to chronic pancreatitis with fibrosis (8). Furthermore, IL-1β was recently shown to enhance PSC activation and is thought to promote pancreatic fibrosis by activating PSCs (19).

Activated PSCs have been shown to secrete cytokines that modulate PSC function, such as activin A (24) and IL-6 (31). Our working hypothesis states that activated PSCs express and secrete IL-1β. Because TGF-β_1 is central to the regulation of PSC function (5, 19), we assume that TGF-β_1 may regulate IL-1β expression and secretion of activated PSCs. We thus conducted this study to assess the regulatory mechanism of IL-1β production in culture-activated PSCs. We report herein that TGF-β_1 enhances IL-1β mRNA expression and peptide secretion by activated PSCs in an autocrine manner. We have further shown, using the adenovirus-mediated double-expression method described above, that a Smad3-dependent, Smad2-independent signaling pathway mediates TGF-β_1-enhanced IL-1β expression and secretion of PSCs. We finally have demonstrated that IL-1β increases TGF-β_1 expression and secretion by PSCs via an ERK-dependent pathway, indicating the existence of an autocrine loop between IL-1β and TGF-β_1 in activated PSCs.

MATERIALS AND METHODS

Materials. TGF-β_1, Nycodenz, pronase, and anti-α-SMA antibody were purchased from Sigma (St. Louis, MO). IL-1β, anti-IL-1β, and anti-TGF-β_1 antibodies were obtained from R&D Systems (Abingdon, UK). DNase I was purchased from Roche (Basel, Switzerland). Collagenase P was obtained from Boehringer Mannheim (Mannheim, Germany). Anti-ERK antibody was purchased from Santa Cruz Biotechnology (Santa Cruz, CA). Antiphosphorylated ERK antibody was obtained from Cell Signaling Technology (Beverly, MA). Horseradish peroxidase (HRP)-conjugated donkey anti-goat IgG, HRP-conjugated donkey anti-mouse IgG, and HRP-conjugated donkey anti-rabbit IgG antibodies were purchased from Jackson ImmunoResearch (West Grove, PA). PD-98059 was obtained from Calbiochem (San Diego, CA).

Isolation and culture of rat PSCs. Rat PSCs were prepared as described previously (4). Briefly, rat pancreas was digested in Gey's balanced salt solution supplemented with 0.05% collagenase P, 0.02% pronase, and 0.1% DNase I. After filtration through nylon mesh, cells were centrifuged in a 13.2% Nycodenz gradient at 1,400 *g* for 20 min. PSCs in the band just above the interface of the Nycodenz solution and the aqueous solution were collected, washed, and resuspended in Iscove's modified DMEM containing 10% FCS, 100 U/ml penicillin, and 100 μg/ml streptomycin. PSCs were cultured in a 5% CO_2 atmosphere at 37°C. All experiments were performed using culture-activated PSCs between *passages* 2 and 3.

Western blot analysis. Western blot analysis was performed as described previously (23) using ECL reagent to visualize secondary antibodies.

Adenoviral infection. Recombinant adenoviruses of Smads were kindly provided by Dr. Kohei Miyazono (University of Tokyo, Tokyo, Japan). For a single adenoviral infection, cells were infected with a recombinant adenovirus at a dose of 10 plaque-forming units (PFU) per cell in the culture media described above. In those experiments using double adenovirus infection, cells were infected with dn-Smad2/3 adenovirus (Ad-dnSmad2/3) at a dose of 10 PFU/cell concomitantly with Smad2 (Ad-Smad2) or Smad3 (Ad-Smad3) adenovirus at doses of 5 or 10 PFU/cell. Subsequent experiments were performed 48 h after infection. An adenovirus expressing β-galactosidase (Ad-LacZ) was used as an infection control.

Measurement of IL-1β and TGF-β_1 peptide secretion. Secretion of IL-1β and TGF-β_1 peptides was measured by determining their concentration in the culture medium using commercially available ELISA kits (Biosource International, Camarillo, CA, and DRG International, Mountainside, NJ) according to the manufacturers' instructions.

RT-PCR. Total RNA was isolated from PSCs using TRIzol reagent (Life Technologies/GIBCO-BRL, Grand Island, NY). First-strand cDNA was made from total RNA using the ReverTra Ace system (Toyobo, Tokyo, Japan) according to the manufacturer's instructions. PCR for TGF-β_1 was performed using a PCR kit for rat TGF-β_1 (Maximbio, San Francisco, CA) according to the manufacturer's instructions. PCR for rat IL-1β and GAPDH was performed using the following primers: rat IL-1β sense, 5′-TCCTAGGAAACAGCAATGGTCG-3′, rat IL-1β antisense, 5′-TTCAT-CCCATACCACGGACAAC-3′; and rat GAPDH sense, 5′-CATGACCAC-AGTCCATGCCATC-3′, rat GAPDH antisense, 5′-CACCCTGTTGCTGTAGCCATATTC-3′. The reactions were conducted using the following

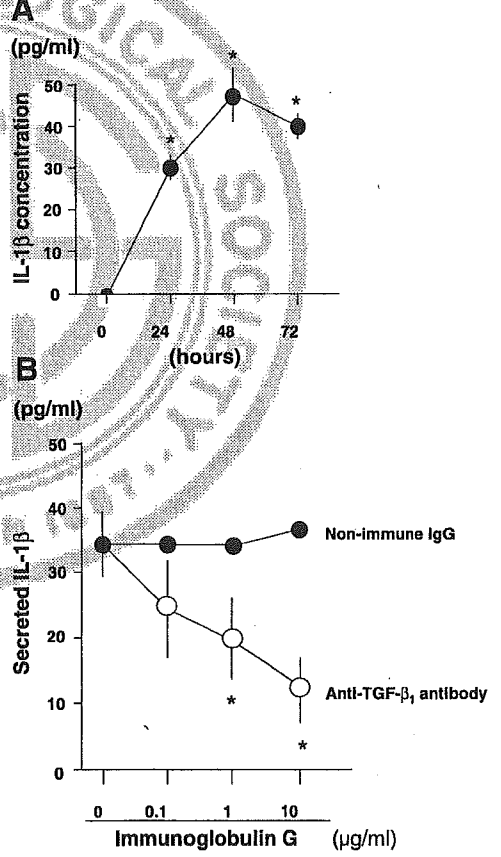

Fig. 1. Anti-TGF-β_1-neutralizing antibody inhibited IL-1β secretion from activated pancreatic stellate cells (PSCs). *A*: IL-1β secretion from PSCs. IL-1β concentration in culture medium was determined by ELISA 1–3 days after the culture medium was changed. Values are means ± SE of 3 independent experiments. *$P < 0.01$ vs. control (*time 0*). *B*: effect of anti-TGF-β_1-neutralizing antibody and nonimmune IgG on IL-1β secretion from PSCs. Concentration of IL-1β secreted from PSCs into culture medium was determined by ELISA after 48-h incubation with indicated amounts of anti-TGF-β_1 antibody (○) or nonimmune IgG (●). Values are means ± SE of 3 independent experiments. *$P < 0.05$ vs. control. AQ: 14

tapraid4/zh0-acel/zh0-acel/zh000406/zh04793d06g | tillotsj | S=5 | 1/7/06 | 2:24 | MS: C-00465-2005 | Ini: 04/PK/BEW | Input-dms

cycle conditions: denaturation at 94°C for 0.5 min, annealing at 45°C for 1 min, and extension at 72°C for 1 min for 30 cycles.

Statistical analysis. The data were analyzed using ANOVA to determine statistical significance, and $P < 0.05$ was considered statistically significant.

RESULTS

IL-1β is secreted from PSCs. We first examined IL-1β secretion from PSCs. As shown in Fig. 1*A*, IL-1β peptide was detected in PSC culture medium. In particular, IL-1β concentration in PSC culture medium was markedly increased after 48-h incubation. No IL-1β activity was detected in fresh culture medium. These data indicate that IL-1β is secreted from PSCs.

Autocrine TGF-β1 stimulates IL-1β secretion from PSCs. Knowing that IL-1β is secreted from PSCs, we next attempted to elucidate the mechanism that regulates IL-1β secretion from PSCs. Because TGF-β1 regulates various functions of PSCs in an autocrine manner (5, 15, 25), we examined the effect of anti-TGF-β1 antibody, which neutralizes TGF-β1 bioactivity, on IL-1β secretion from PSCs. As shown in Fig. 1*B*, anti-TGF-β1 antibody decreased IL-1β secretion from PSCs in a dose-dependent manner, indicating that autocrine TGF-β1 enhances IL-1β secretion from PSCs.

Exogenous TGF-β1 increased IL-1 expression and secretion by PSCs. As an independent experiment to examine the effect of TGF-β1 on IL-1β secretion from PSCs, we added exogenous TGF-β1 to PSC culture medium and determined secreted IL-1β from PSCs. Because maximal IL-1β secretion from PSCs was observed in 48-h incubation, we first examined the effect of TGF-β1 on IL-1β expression and secretion at this time point. As shown in Fig. 2, exogenous TGF-β1 enhanced IL-1β mRNA expression in PSCs (Fig. 2*A*). In addition, exogenous

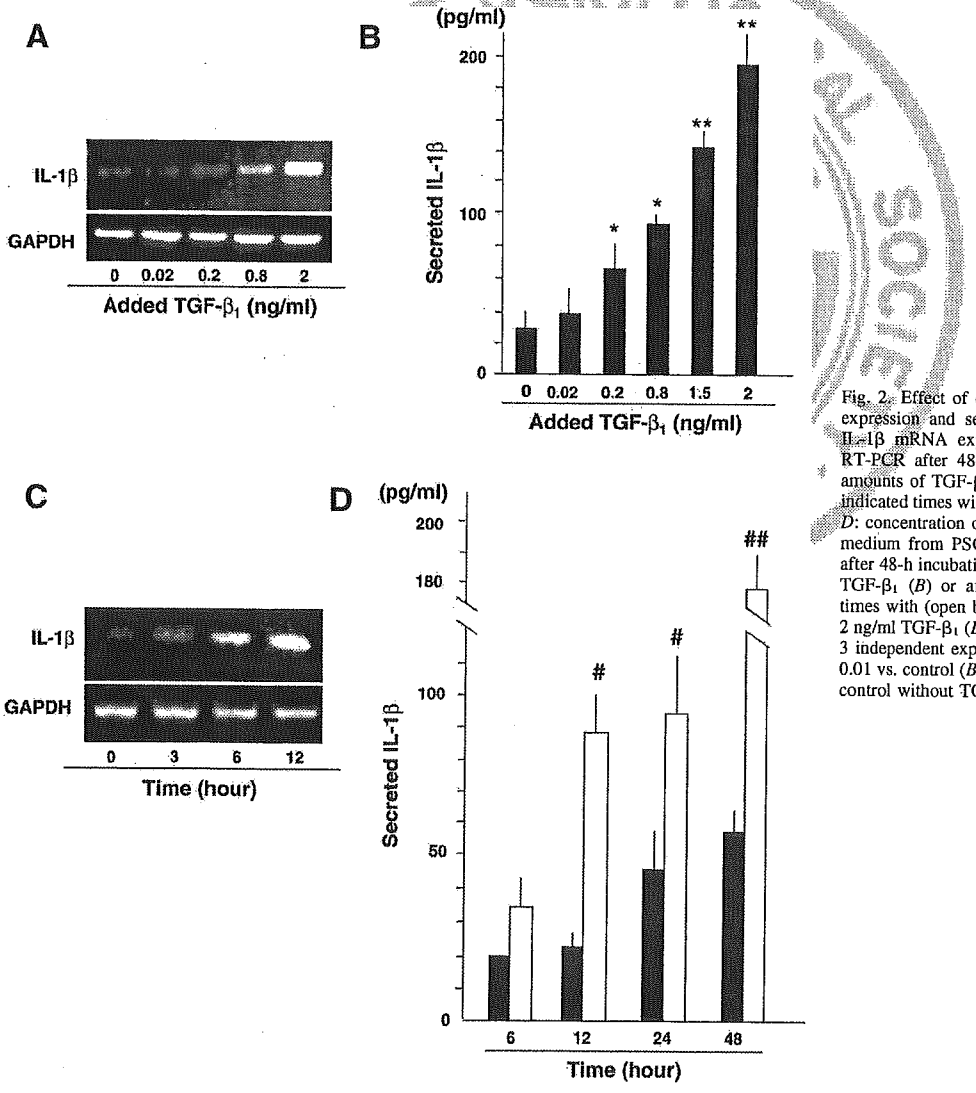

Fig. 2. Effect of exogenous TGF-β1 on IL-1β expression and secretion by PSCs. *A* and *C*: IL-1β mRNA expression was determined by RT-PCR after 48-h incubation with indicated amounts of TGF-β1 (*A*) or after incubation for indicated times with 2 ng/ml TGF-β1 (*C*). *B* and *D*: concentration of IL-1β secreted into culture medium from PSCs was quantified by ELISA after 48-h incubation with indicated amounts of TGF-β1 (*B*) or after incubation for indicated times with (open bars) and without (solid bars) 2 ng/ml TGF-β1 (*D*). Values are means ± SE of 3 independent experiments. $*P < 0.05$, $**P < 0.01$ vs. control (*B*). $\#P < 0.05$, $\#\#P < 0.01$ vs. control without TGF-β1 (*D*).